12 July 1968, Volume 161, Number 3837 SCIENCE

Bonding and Structures of Transition Metals

Spectroscopy of gaseous atoms provides predictions of structures and thermodynamic properties of metals.

Leo Brewer

The great variety of structures and combining ratios in intermetallic compounds offers a challenge to bonding theories. Can the compositions and structures of these intermetallics be correlated and explained in terms of the same principles used for chemical substances generally?

For all substances it is the interactions of electrons with the nuclei which constitute the glue that binds atoms together, and any explanation of the structures, compositions, and stabilities of intermetallic compounds must be based upon the same principles of electronic interactions that apply to all materials.

Valence Bonds and Molecular Orbitals

The common approaches to the description of electronic bonding are termed the molecular-orbital and valence-bond methods (*1*). The molecular-orbital method starts with the atomic nuclei already assembled in the molecule or solid; electrons are added to molecular orbitals in an *aufbau* (building-up) process patterned after the *aufbau* process for free atoms. The valence-bond approach starts with the electrons associated with separated atoms, either in the ground electronic states or in low-lying excited electronic states; electron-pair bonds form between the nuclei as the atoms approach. The methods become equivalent (*2*) if they are used in full complexity. However, at a practical level of approximation, each method has serious deficiencies. The simple molecular-orbital method underestimates and the simple valence-bond method overestimates electron correlation due to the coulombic repulsion of the electrons in an electron-pair bond. The molecular-orbital method breaks down for large internuclear distances, but it has the advantage of more readily providing information about the excited electronic states of a molecule. Molecular-orbital theory has been extensively used in recent years for conjugated and aromatic molecules and has been the most common approach to metallic bonding through use of the electron-band model. However, the bulk of chemical bonding experience has been expressed in terms of electron-pair bonding. Although the electrical and magnetic properties of metals (which are largely characterized by the density of electronic levels near the Fermi surface) are most satisfactorily described by the molecular-orbital approach, an extension of the valence-bond approach used for metals by Pauling (*3*) as modified by Engel (*4*), is the most practical way at present to relate the chemical behavior of all materials to the understanding of the structures, composition ranges, and thermodynamic stabilities of the phases of metallic systems.

Nonmetals

The application of the valence-bond method to nonmetals is familiar to most scientists. Thus chlorine atoms with the electronic configuration s^2p^5 in the valence shell form diatomic molecules with one electron-pair bond per atom; sulfur (s^2p^4) forms rings or linear chains with two electron-pair bonds per atom; and phosphorus (s^2p^3) forms three electron-pair bonds per atom in the puckered graphite-like structure of black phosphorus or in the tetrahedral P_4 molecule found in the gas and in white phosphorus. Because a *p* orbital can accommodate only six electrons divided into two groups of opposing spins, the structures are fixed by the number of unpaired electrons in the free atom.

The ground electronic configuration of silicon (s^2p^2) has only two unpaired electrons, but the excited configuration (sp^3) with four unpaired electrons is sufficiently close to the ground state so that the promotion energy (*5*) of 95 kilocalories per gram atom (required to unpair the two *s* electrons of the ground electronic configuration by excitation to the sp^3 configuration) is less than the bonding energy due to the additional two electron-pair bonds which can be formed by the sp^3 configuration. Thus silicon forms the diamond structure with each atom bonded to four other atoms.

The common feature of these examples is the correlation of molecular structure with electronic configuration because the number of bonds per atom is limited by the number of unpaired electrons per atom. When, as for the fourth-group elements, a relatively low-lying electronic configuration which has more unpaired electrons than the ground configuration is available, the excited or promoted configuration will

---

The author is professor, department of chemistry, and head of the inorganic materials research division, Lawrence Radiation Laboratory, University of California, Berkeley.

Table 1. Crystal structures of metals. I represents body-centered cubic; II, hexagonal close-packed; and III, cubic close-packed. The structures are listed in order of temperature stability with the room-temperature structure lowest.

Na I	Mg II	Al III									
K I	Ca I III	Sc I II	Ti I II	V I	Cr I	Mn I III β χ	Fe I III I	Co III II	Ni III	Cu III	Zn II
Rb I	Sr I II III	Y I II	Zr I II	Nb I	Mo I	Tc II	Ru II	Rh III	Pd III	Ag III	Cd II
Cs I	Ba I	La I III II	Hf I II	Ta I	W I	Re II	Os II	Ir III	Pt III	Au III	

dominate the bonding and the structural characteristics. From chlorine to silicon the atomization enthalpies (the enthalpy required to break the bonds of the solid so as to produce gaseous atoms in the ground electronic state) are 32, 67, 80, and 109 kilocalories per gram atom, respectively.

Nontransition Metals

The valence-bond theory can also be applied to metals to determine the number of electron-pair bonds per atom. The principal difference between metals and nonmetals is that the nonmetallic elements make maximum use of their orbitals and fill all eight positions in the *s* and *p* orbitals through the formation of localized electron-pair bonds. Metals do not have enough electrons to make full use of their *s* and *p* valence orbitals. The availability of vacant orbitals allows the electrons to become somewhat delocalized; thus the electrical conductivity characteristic of metals occurs.

Sodium, magnesium, and aluminum, the metals of the third row of the periodic table, will be taken as examples. Sodium, with one $3s$ valence electron, can form only one electron-pair bond per atom, but this bond is spread out over the eight nearest neighbors and the six next nearest neighbors and even the more distant neighbors of the body-centered cubic (bcc) structure. Magnesium, with the ground electronic configuration $3s^2$, would not be able to form any electron-pair bonds if it were not for the comparatively low energy of the next excited configuration $3s3p$. The promotion energy (*5*) of 63 kilocalories per gram atom, necessary to excite the $3s^2$ configuration to $3s3p$, is small enough to be offset by the bonding energy of 98 kilocalories per gram atom provided by the two unpaired electrons of the $3s3p$ configuration; the two electron-pair bonds are spread among the 12 nearest neighbors and more distant neighbors of the hexagonal close-packed (hcp) structure. For aluminum 83 kilocalories per gram atom must be used to promote the s^2p to the sp^2 configuration so as to make full use of the valence electrons; the three electron-pair bonds per atom of aluminum are spread among the 12 nearest neighbors and more distant neighbors of the cubic close-packed (ccp) structure. The atomization enthalpies for sodium, magnesium, aluminum, and silicon are 26, 35, 78, and 109 kilocalories per gram atom, respectively.

The three general principles that were illustrated in the application of valence-bond theory to both metallic and nonmetallic elements of the third row of the periodic table are: (i) the number of electron-pair bonds per atom associated with a given electronic configuration of the element is determined by the number of unpaired electrons of the free atom; (ii) low-lying electronic configurations with more unpaired electrons than the ground electronic configuration may predominate if the bonding energy from the additional electron-pair bonds offsets the promotion energy of the excited state; and (iii) each bonding configuration produces a characteristic, stable, solid structure.

Transition Metals

For the fourth row or first long period of the periodic table, the metallic state does not end with the fourth valence electron at titanium but continues through the first transition series and ends with the 14th valence electron at germanium. Examination of the spectroscopic data (*5*) for the gaseous atoms indicates that the $3d$ orbitals are close in energy to the $4s$ and $4p$ orbitals. Until these $3d$ orbitals have been filled, it is not possible to fill up the *s* and *p* orbitals to achieve the sp^3 configuration which produces the nonmetallic diamond structure.

In Table 1 (*6*) the crystal structures of the stable solid forms of the metallic elements to be discussed are listed. When an element undergoes transformation upon heating above room temperature, the lowest structure is the room-temperature form, with the order of structures given in order of occurrence with increasing temperature. The bcc structure of the alkali metals with one valence electron is designated as structure I. The hcp structure of magnesium is designated as structure II. The ccp structure of aluminum is designated as structure III. This nomenclature has been chosen to emphasize the correlation (*4*) between the occurrence of these three structures and the presence of one, two, or three bonding electrons of the *s,p* type, respectively. The simple sequence of structures I, II, and III (Table 1) that we observed for sodium, magnesium, and aluminum is more complicated for the transition metals. Structure I (bcc) is observed for all of the metals of the first six columns of the three transition series, although only as the high-temperature form for some of the metals.

On going to the right, structure II (hcp) is observed for metals of the seventh and eighth columns of the second and third transition series, and structure III (ccp) is observed for all of the transition metals to the right. Although the data were less complete then, Engel (*4*) suggested that this sequence could be understood on the hypothesis that the structures were determined by the number of *s,p* electrons and that structure I (bcc) of the alkali metals persisted up to molybdenum and tungsten because the *d* orbitals act as a sink for the electrons beyond the one *s* electron until the d^5s configuration is reached. Calculations (*7*) have indicated that mixing of *d* orbitals with *s* and *p* orbitals results in hybrid orbitals with spatial arrangements in agreement with the Engel correlation. A more definitive proof of the Engel correlation can be given from examination of the spectroscopic data (*5*) for the gaseous atoms.

Qualitative Test of Engel Correlation

An analysis of the spectra of the transition elements of the first six groups reveals (*5*) that the low-lying electronic configurations are of the type $d^{n-2}s^2$, $d^{n-1}s$, and $d^{n-2}sp$, where n is the total number of $(d + s + p)$ valence electrons, with d^n, $d^{n-1}p$, $d^{n-3}s^2p$, and $d^{n-3}sp^2$ somewhat higher in energy. For elements of the first six groups, $d^{n-1}s$ and $d^{n-2}sp$ are the lowest configurations with all of the electrons unpaired and available for bonding. Comparisons of promotion energies and bonding energies indicate that these two configurations should be the most important bonding configurations. For reasons of space, these comparisons will be largely restricted to metals of the second transition series, rubidium through silver; the reader is referred to more detailed discussions (*6, 8*) for similar comparisons for metals of the first and third transition series.

The relative energies (*5*) of the $d^{n-1}s$ and $d^{n-2}sp$ configurations for the gaseous elements of the second transition period (strontium to molybdenum) are illustrated in Fig. 1. The energies of each configuration are presented as bands because there are, in general, several spectroscopic states for each electronic configuration, corresponding to different combinations of the spin and orbital momenta of the electrons. The range of energies of spectroscopic states of highest spin multiplicity (spin momenta combined with minimum pairing) corresponding to each of the electronic configurations is shown in Fig. 1. In general, the *d* orbitals, which are in an inner shell, become stabilized with respect to the *s* and *p* orbitals of the outer shell as the nuclear charge increases from left to right in a transition metal period. For strontium, yttrium, and zirconium the $d^{n-1}s$ and $d^{n-2}sp$ configurations are close enough in energy that both configurations would be expected to be important; by the Engel correlation both structures I and II, corresponding to configurations $d^{n-1}s$ and $d^{n-2}sp$, would be expected. For niobium and molybdenum the $d^{n-1}s$ configuration has become so much lower in energy than the $d^{n-2}sp$ configuration that one would expect structure II (hcp) to be unstable. Both configurations have the same number of bonding electrons; thus the large difference in promotion energy cannot be compensated by additional bonding energy as in the example of magnesium, where the excited *sp* configuration with two bonding electrons predominates over the s^2 configuration with no bonding electrons.

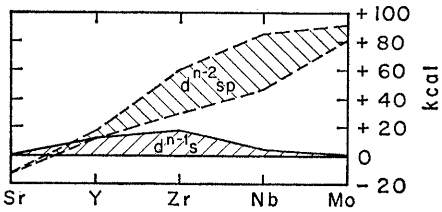

Fig. 1. Relative energies of the $d^{n-1}s$ and $d^{n-2}sp$ electronic configurations for gaseous atoms of the second transition series in kilocalories per gram atom.

Table 1 shows that niobium and molybdenum exhibit only the bcc structure at all temperatures and at the highest pressures available, in agreement with the Engel correlation; for strontium, yttrium, and zirconium the bcc structure is stable at high temperatures and transforms to the hcp structure at lower temperatures. Recent observations (*9*) indicate that, for strontium, small amounts of hydrogen may be necessary to stabilize the hcp structure, but the energies of the bcc and hcp phases must be very close. The greater lattice vibration of the bcc structure with lower coordination number produces a higher entropy, which is the requirement for high-temperature stability when two structures have comparable energies. The only exception to this general behavior occurs in the case of iron, where differences in the magnetic contributions to the entropy at lower temperatures are greater than differences in vibrational contributions; this permits bcc iron to transform to ccp over a short temperature interval before reverting back to the bcc structure at higher temperatures (*10*).

Basis of the Engel Correlation

The structure of each nonmetal is clearly correlated with the total number of *s,p* valence electrons per atom. The extension of this concept to metallic systems was first made by Hume-Rothery (*11*), who noted that many varied intermetallic compounds with the same average number of valence electrons per atom had the same crystal structure. This very important concept —phases of characteristic structure associated with a limited range of concentrations of electrons per atom—implies that if excess free energy is plotted against composition or against valence electron concentration the curve must turn up rather steeply at certain limiting electron concentrations. From examination of alloy systems, where the bonding is due to *s,p* electrons only, structure III (ccp) can be correlated with a range of approximately 2.5 to 3 *s,p* electrons per atom. For structure II (hcp) the free energy rises steeply beyond the limits of 1.7 to 2.1 *s,p* electrons per atom, and the structure I (bcc) is limited to a concentration of less than 1.5 *s,p* electrons per atom. Other crystal structures can also be correlated with characteristic electronic concentration ranges. The transition metals have been stumbling blocks to the more general application of the Hume-Rothery rules because of uncertainty about the valence. The use of the total number of valence electrons with the *d* electrons included did not yield consistent predictions.

The Engel correlation, which uses only the *s,p* electrons in correlations between structure and electronic concentration, now allows an extension of the Hume-Rothery rules to the transition metals. Why is the structure determined only by the *s,p* electrons and not by the *d* electrons? The *d* electrons play an important role in determining structure indirectly. A consideration of the relative stabilities of *d, s,* and *p* electrons in the gaseous atoms and the energy resulting from electron-pair bonding of the unpaired electrons determines how many *s,p* electrons are available for bonding.

The relative roles of the *d* and *s,p* electrons can be exemplified by the condensation of gaseous tungsten atoms in their d^4s^2 ground state to the liquid state. The promoted configuration, d^5s, with six electrons available for bonding, predominates in the liquid, with the five *d* electrons contributing over 150 kilocalories to the bonding energy while the contribution of the *s* electron is only 54 kilocalories. As the temperature is lowered to produce the solid, the major contributors to the cohesive energy, the localized *d* bonds, do not influence long-range structure, but the far-ranging *s* electron bonds do establish the body-centered cubic structure. Thus the Engel correlation implies that once the *d* electrons have determined promotion energies and bonding energies, the crystal structure is fixed by the concentration of the remaining *s,p* electrons. It has been noted above (*7*) that a hybrid mixture of one *s* orbital with varying numbers of *d* orbitals could produce structure I (bcc); similar results are obtained for the relation between $d^{n-2}sp$ and the hcp structure.

An alternative rationalization of the Engel correlation can be offered in terms of nonhybridization. In contrast to ion complexes of transition metals, where *s* and *p* electrons are somewhat localized and thus can often form good hybrid bonds with *d* electrons, the *s* and *p* electrons in a metal are greatly delocalized; they have become an electron gas. The *d* electrons, which belong to an inner electron shell, are much more localized and cannot obtain good overlap with *s* and *p* electrons. The main *d* bonding contribution appears to come from *d-d* bonding. In terms of band theory, the *d* bands are somewhat separated from the *s,p* or metallic electron bands. If the *d* electrons are localized to bonds with only nearest neighbors, whereas the *s,p* electrons range far out into the metal, it is not unreasonable to assign the determination of long-range structure to the *s,p* electron concentration.

The quantitative test of the Engel correlation for pure metals as well as the extension to alloy systems to be given below will be based on the occurrence of structure I (bcc) up to $sp^{0.5}$ or a maximum of 33 percent *p* character for the metallic or *s,p* electrons. Structure II (hcp) will be associated with the range $sp^{0.7-1.1}$ or 41 to 52 percent *p* character for the metallic electrons. Structure III (ccp) will be correlated with $sp^{1.5-2}$ or 60 to 67 percent *p* character for the metallic electrons. By contrast, the sp^3 configuration of the diamond structure has 75 percent *p* character.

It is not immediately obvious whether the number of metallic (*s,p*) electrons per atom or the percent *p* character of the metallic electrons would be the decisive factor in determining long-range structure. In the application of the Engel correlation, either could be used since almost all effectively bonding electronic configurations have essentially one *s* electron per atom, and there would be a one-to-one correspondence between the number of *s,p* electrons per atom and the percent *p* character of the metallic electrons. There is one situation where there would be a distinction. At the beginning of each period, the closed electronic shells are rather expanded and easily distorted or polarized. Upon moving to the right in the periodic table, the increasing nuclear charge rapidly causes a contraction of the shell and closed-shell polarization effects should become negligible after the alkali and alkaline-earth metals. Pauling (*3*) estimated considerable *p* character in the alkali metals and diatomic molecules due to hybridization between *s* and *p* orbitals. Recent pseudopotential calculations (*12*) suggest that polarization of the closed electronic shell of sodium plays a significant role in the bonding and that there is considerable mixing of closed-core *p* electrons with the *s* valence electrons which serves to increase the *p* character of the bonding electrons even more than considered by Pauling. The anomalous occurrences of certain structures to be discussed below indicate that possibly the percent *p* character may be the controlling factor. However, this ambiguity exists only for the alkali and alkaline-earth metals and can be ignored for the other transition metals. In the application of the Engel correlation, the number of *s,p* electrons per atom will be considered decisive.

Quantitative Application of Engel Correlation

We can now use the Engel correlation in a more quantitative manner to allow prediction of the thermodynamic properties of bcc and hcp structures even when they are not observed for the pure element. For all of the transition metals except rhodium and palladium, atomic spectroscopy has yielded (*5*) complete data on the relative energies of the $d^{n-1}s$, $d^{n-2}sp$, and $d^{n-2}s^2$ electronic configurations, where *n* is the total number of valence electrons. The experimental (*13*) heats of atomization of the metals given in Table 2 correspond to the ground electronic state of the gaseous atom, which is often the $d^{n-2}s^2$ state. The spectroscopic data al-

Table 2. Heats of atomization of solid elements (*13*) in kilocalories per gram atom at 298.15°K or at the melting point, whichever temperature is lower.

Na 25.9	Mg 35	Al 78											Si 109	P 80 ± 10	S 66	Cl 32.2	Ar 1.85
K 21.5	Ca 42.5	Sc 90	Ti 112	V 123	Cr 95	Mn 68	Fe 99.3	Co 102.4	Ni 102.8	Cu 81.1	Zn 31.2	Ga 66	Ge 89.5	As 72 ± 3	Se 54	Br 28.1	Kr 2.57
Rb 19.5	Sr 39	Y 101.5	Zr 145.5	Nb 172	Mo 157	Tc 158	Ru 153	Rh 133	Pd 91	Ag 68	Cd 26.7	In 58	Sn 72	Sb 63	Te 48	I 25.5	Xe 3.57
Cs 18.7	Ba 42.5	La 103	Hf 148	Ta 187	W 203	Re 187	Os 188	Ir 160	Pt 135	Au 88	Hg 15.3	Tl 44	Pb 47	Bi 49.5	Po 34.5		

Table 3. Bonding energies in kilocalories per gram atom of the $d^{n-2}sp$ valence state in the hexagonal close-packed structure. Asterisks indicate that bonding energy is given for the $d^{n-1.7}sp^{0.7}$ valence state. The number of bonding electrons per atom for Ru*, Rh*, and Pd* are 5.4, 4.4, and 3.4, respectively. For Cu*, Ag*, and Au*, the $d^{9.3}sp^{0.7}$ valence state has 2.4 bonding electrons per atom. The method of calculating nonintegral electronic configurations corresponding to the minimum energy is given by Brewer (*8*). Values in parentheses are predicted values for unstable structures.

Number of bonding electrons per atom													
2	3	4	5	6	7	6		5		4		2.4	2
Mg 98													
Ca (85)	Sc 135	Ti 157	V (165)	Cr (158)	Mn (120)	Fe 153		Co 169		Ni (171)		Cu* (135)	Zn 124
Sr 80	Y 144	Zr 188	Nb* (197)	Mo* (198)	Tc 205		Ru* 204		Rh* (189)		Pd* (165)	Ag* (130)	Cd 144
Ba* (74)	La* 132	Hf 199	Ta (231)	W (244)	Re 241	Os 255		Ir (234)		Pt (215)		Au* (140)	Hg (123)

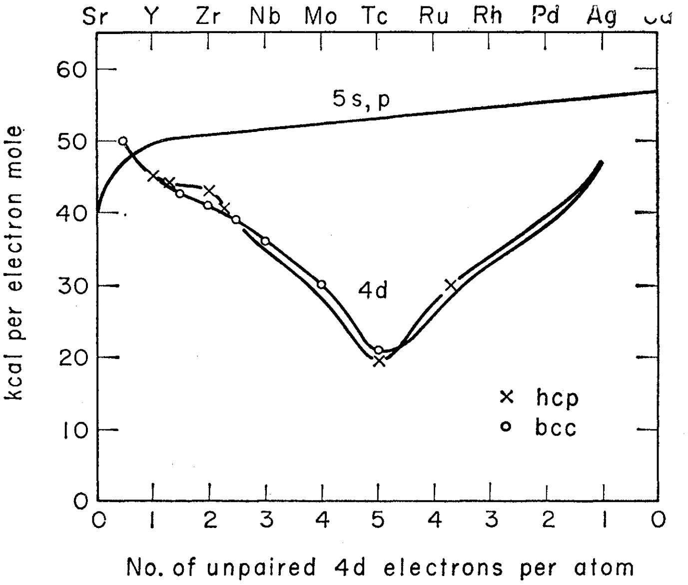

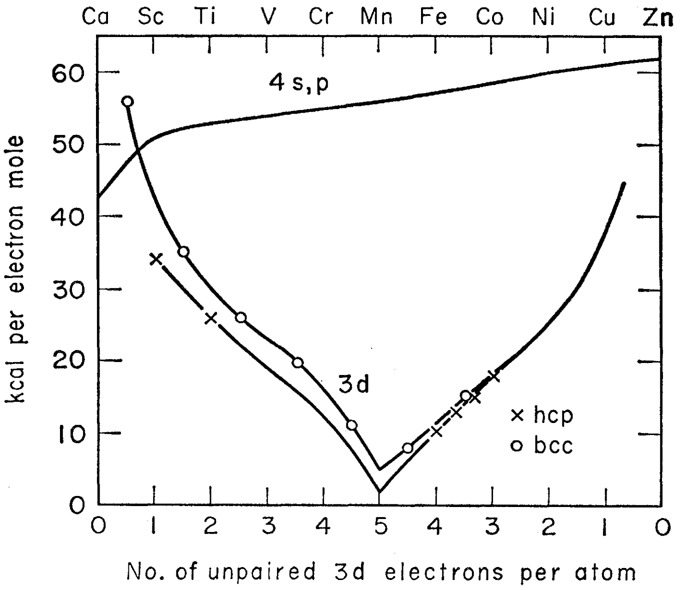

Fig. 2 (left). Valence-state bonding enthalpy per unpaired electron in kilocalories per gram atom. In the upper curve bonding enthalpy of *5s* or *5p* electrons is plotted for each element. The bottom curve plots bonding enthalpy of *4d* electrons against number of unpaired *d* electrons. Fig. 3 (right). Valence-state bonding enthalpy per unpaired electron in kilocalories per gram atom. The upper curve plots bonding enthalpy of *4s* or *4p* electrons for each element. In the bottom curve is plotted the bonding enthalpy of of *43d* electrons against the number of unpaired *d* electrons.

low calculation of the energy difference between the metallic state and the bonding valence states $d^{n-2}sp$ and $d^{n-1}s$, depending upon the structure. For scandium 90 kilocalories per gram atom for vaporization of the solid to atomic scandium (d^2s), and 45 kilocalories per gram atom for promotion to *dsp*, yield a valence state bonding energy of 135 kilocalories per gram atom. Table 3 shows the bonding energy (*8*) of the $d^{n-2}sp$ valence state in the hcp structure or the energy required to vaporize the metal in the hcp structure to gaseous atoms in the $d^{n-2}sp$ state. Composition ranges for alloys show that each structure occurs over a finite range of electron concentrations. It is possible to calculate (*8*) the minimum energy within each range to fix the effective electronic concentration as indicated in Table 3. Similar tables can be prepared for the bonding energy of the bcc structure from its valence state. These bonding energies are due in part to the bonding of *s* and *p* electrons and in part to the bonding of *d* electrons.

Figure 2 shows the variation for *4d* metals due to increasing nuclear charge of the bonding energy for one *s* or *p* electron which has been estimated (*8*) from the known bonding energies for strontium and cadmium. The average value given by the 5 *s,p* curve is used for either *s* or *p* electrons. The *s* and *p* contributions have been subtracted from the total bonding energies, such as those tabulated in Table 3, to yield the resulting bonding energy per electron for the *d* electrons. The abscissa for the *s,p* curve represents increasing atomic number, indicated by the atomic symbol; the abscissa for the *d* curve is the number of unpaired *d* electrons available for bonding. Data which are given for both the bcc and hcp structures indicate that the bonding energy of a *d* electron decreases as more and more electron-pair bonds are crowded around an atom until a minimum in the bonding energy per electron is reached when five *d* electrons per atom are used for bonding and that the same smooth curve can be used to estimate values for either the bcc or hcp structures.

The characteristic variation of *d* electron bonding with the number of *d* electrons is found (*8*) also for the first and third transition periods. The major difference is the very pronounced increase in the bonding effectiveness of the *d* electron upon going down in the periodic table from the first to third transition series. This trend is opposite to the general decrease in *s,p* bonding effectiveness with increasing internuclear distances upon going down in the periodic table. For metals of the second and third transition series, the *d* electrons can be used so effectively in electron-pair bonds that no electrons are left unpaired. Since unpaired *d* electrons are required for magnetism, the metals of the second and third transition series are not magnetic. For the metals chromium to nickel of the first transition series, the relative ineffectiveness of the *d* electron bonding with spin-pairing can be seen by comparing Fig. 3 with Fig. 2. For these metals the bonding energy that could be obtained by concentration of an electron pair between the nuclei is offset by the reduced coulombic repulsion between unpaired electrons. The fact that some of the *d* electrons are left unpaired causes these metals to be magnetic.

With the exception of manganese, all 32 transition metals exhibit only the bcc, hcp, or ccp crystal structures. The minor distortions or modifications of the hcp form that occur in a few instances can be neglected. How well do the observations fit the predictions of the Engel correlation? Spectroscopic data for the $d^{n-1}s$ and $d^{n-2}sp$ configurations, which are correlated to structure I and structure II, respectively, are sufficiently complete to allow predictions of the stabilities of these structures on a qualitative basis as outlined in connection with the discussion of Fig. 1. Quantitative predictions of relative stabilities are derived through comparison of bonding energies of *d* with *s,p* electron-pair bonds, as given in Figs. 2 and 3, together with the spectroscopic promotion energies. Table 4 summarizes (*8*) the quantitative predictions by tabulating values for the heats of sublimation (ΔH°_{298}) to the ground electronic state of the gaseous atom for the bcc and hcp forms of most of the transition metals. The values in parentheses are predicted values for structures which are not observed as stable phases. The calculations of Table 4 are based on spectroscopic data for the gaseous atoms and on the Engel correlation between electronic configuration and crystal structure; in all instances where calculations indicate that a structure is unstable by 2 kilocalories per gram atom or more, the experimental observations summarized in Table 1 confirm that the predicted unstable structure is not found to be stable at any temperature or at any pressure that has been used. There are 11 instances where the bcc and hcp structures have enthalpies within 1 kilocalorie of each other. Strontium, yttrium, and zirconium have already been discussed in conection with Fig. 1. For scandium, titanium, lanthanum, and hafnium, where the bcc structure has a higher enthalpy than the hcp structure by 1 kilocalorie, the hcp structure is stable, but transforms to the bcc structure at higher temperatures because of the higher entropy of the bcc structure (for reasons given in the discussion of the high-temperature stability of the bcc phase of strontium, yttrium, and zirconium). For calcium, where the calculations indicate the same enthalpy for both bcc and hcp structures, the hcp structure is unstable with respect to the bcc phase of higher entropy but can be stabilized by small additions of hydrogen (*14*). Manganese occupies a unique situation in that all three electronic configurations yield comparable stabilities. As a result, manganese forms the complex α-Mn and β-Mn structures, designated as χ and β in Table 1; these structures are known for a number of binary and ternary systems with atoms of different sizes to meet the packing requirements for atoms of different size in different sites. Because of the availability of three electronic structures of comparable stability, manganese is able to provide the atoms of different size itself by assuming different electronic structures depending upon the crystal site. Uranium and plutonium appear to provide two additional examples of this type of behavior.

For nickel and iron the bcc structure is calculated to be more stable than the hcp structure by 1 kilocalorie per gram atom. The hcp structure of iron is unstable with respect to the bcc structure, but it is stabilized by 110 kilobars at 490°C. The bcc and hcp forms of nickel are calculated to be unstable with respect to the ccp form by 5 kilocalories per gram atom and only the ccp structure is observed.

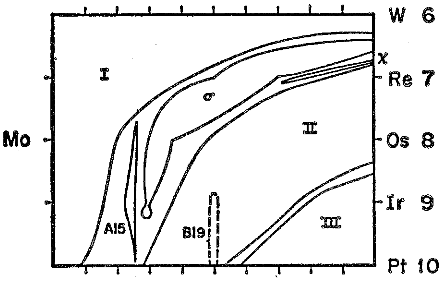

Fig. 4. Multicomponent phase diagram of molybdenum with third transition series metals, projected along the temperature axis. Abscissa gives atomic percent of molybdenum in alloys.

The spectroscopic data for the $d^{n-3}sp^2$ configuration are not complete enough for quantitative calculations of the enthalpies of the ccp phases. However, the heats of sublimation for the ccp phases of manganese, iron, and the metals of the ninth, tenth, and eleventh groups are known. Comparison of these values with the calculated values for the bcc and hcp phases shows that the ccp phase is the only one observed when the calculated heats of sublimation of the bcc and hcp phases are smaller than the values for the ccp phase. For manganese, iron, and cobalt, where several structures have almost the same enthalpy, the values are consistent with reasonable estimates of the $d^{n-3}sp^2$ promotion energies based on the observed energies required to promote d electrons to p electrons for other electronic configurations.

The bcc and ccp structures are found for manganese and iron but not for technetium, rhenium, ruthenium, and osmium, the corresponding metals of the seventh and eighth groups of the second and third transition series. The higher energies required for the promotion of d to p electrons for technetium, rhenium, ruthenium, and osmium are primarily responsible for the instability of the ccp structure. The bcc structure is unstable with respect to the hcp structure for the second and third transition series mainly because of the much higher bonding ability of the d electrons. A transformation from hcp ($d^{n-2}sp$) to bcc ($d^{n-1}s$) for metals of the seventh group or beyond would cause loss of two bonding electrons (one d and one p).

The stability of the ccp structure for the ninth, tenth, and eleventh groups is consistent with the Engel correlation; the bonding energies shown in Fig. 2 indicate that the expected energies necessary for the d to p promotion are more than offset by the additional d and p electron-pair bonds to yield bonding states with promotion at least to $d^{n-2.5}sp^{1.5}$. For example, the promotion of two d electrons per gold atom from ($d^{10}s$) to (d^8sp^2) would increase the number of electrons available for electron-pair bonding from one to five electrons per atom. All of these electrons would be spin-paired in the formation of electron-pair bonds; the d orbitals would be completely occupied. Likewise, the s and p electrons would be spin-paired in the usual manner of metallic s,p electrons.

For metals of the fourth to sixth groups, even rough estimates of the promotion energies of the $d^{n-3}sp^2$ configuration together with bonding energies calculated from plots such as those of Figs. 2 and 3 are sufficient to clearly predict the instability of the ccp structure. Accurate spectroscopic data for yttrium predict that the ccp structure is unstable by 20 kilocalories per gram atom relative to hcp or bcc yttrium. The spectroscopic data for scandium and lanthanum are too incomplete for accurate calculations of the thermodynamics of the ccp structure.

The explanation for the increase of bonding strength of d electrons from the first to third periods(given above in terms of poor overlap of $3d$ orbitals) is an important concept for predicting the stabilities of intermetallic compounds. Metals of the first transition series with poor d orbital overlap are greatly stabilized in structures, such as the A15 or V_3Si structure, which tend to squeeze the atoms abnormally closely. Likewise the effect of compression through application of external pressure can be predicted on the basis that compression improves the bonding ability of the poorly overlapping d orbitals more strongly than the s or p orbitals. Thus the application of pressure would stabilize the structure with the greatest number of bonding d electrons relative to other structures. For the transition metals of the first six groups, the bcc structure with $d^{n-1}s$ configuration has the most bonding d electrons according to the Engel correlation and would be stabilized by pressure with respect to the hcp or ccp structures even though these close-packed structures have higher coordination numbers. This requires that the bcc structure for the first six groups must be more dense or at least more compressible, and therefore more dense under pressure, than the close-packed structures. The data for titanium, zirconium, and hafnium are in agreement (*15*). On this same basis, the close-packed structures of the fifth- and sixth-group metals will not be stabilized by pressure. For transition metals beyond the sixth group, the $d^{n-1}s$ configuration will have fewer bonding *d* electrons than the hcp or ccp configurations which correspond to promotion of paired *d* electrons to unpaired *p* electrons. Thus pressure should favor the hcp structure over the bcc structure beyond the sixth group and should favor the ccp structure over the hcp structure beyond the seventh group. Fragmentary data based on high-pressure measurements (*15*) are largely in agreement with the predictions based on the Engel correlation.

Table 4. Heats of sublimation in kilocalories per gram atom of body-centered cubic and hexagonal close-packed phases of the transition metals. Values in parentheses are predicted values for unstable structures.

	Ca	Sc	Ti	V	Cr	Mn	Fe	Co	Ni	Cu
bcc	42	89	111	123	95	67	99	(100)	(98)	(61)
hcp	(42)	90	112	(118)	(87)	(67)	(98)	102	(97)	(56)
	Sr	Y	Zr	Nb	Mo	Tc	Ru	Rh	Pd	Ag
bcc	38	101	145	172	157	(152)	(151)	(131)	(83)	(56)
hcp	39	102	146	(163)	(142)	158	153			
	Ba	La	Hf	Ta	W	Re	Os	Ir	Pt	Au
bcc	43	102	147	187	203	(184)	(177)	(155)	(124)	(59)
hcp	(41)	103	148	(182)	(189)	187	188	(159)	(129)	(55)

Contradictions to Engel Correlation

Of the 99 possible predictions for the three structures of the 33 metals of the three transition series, the only two clear contradictions are the occurrence (*9, 14*) of ccp phases at low temperature for calcium and strontium. The Engel correlation would require at least 2.5 *s,p* bonding electrons per atom with at least 60 percent *p* character. Outside the group of 33 transition metals, a few additional exceptions are known. For example, the occurrence (*16*) of hcp phases of lithium and sodium at very low temperatures would require at least 1.7 *s,p* electrons per atom with at least 41 percent *p* character in order to be consistent with the Engel correlation. It has been suggested (*7*) that these occurrences are related to the anomalous order of stability for the rare gas structures. The discussion above, in the section headed Basis of the Engel Correlation, has indicated that polarization of the closed electronic cores of the alkali and alkaline-earth metals, which serves to increase the *p* character of the valence electrons, may be the significant factor responsible for the anomalies. Whether this is the correct explanation or not, the anomalous structures are found only with weakly bonded materials near the beginning of a period, and the factor responsible need not be considered for the remainder of the metals.

Multicomponent Phase Diagrams

As for the pure metal, the electronic configurations are the primary factors that fix the thermodynamic and structural properties of intermetallic phases. However, it is necessary also to consider the effect of size differences of the component atoms, internal pressure differences, and charge transfer.

In structures with all lattice sites equivalent, the mixing of atoms of different sizes tends to reduce thermodynamic stability. On the other hand, there are a number of structures characteristic of intermetallic phases, such as the α-Mn (or χ), the β-Mn, and the β-U (or σ) structures, for which different volumes are available at different crystal sites and a mixture of atoms of different sizes is required for maximum stability. The internal pressure, which is commonly evaluated from the quotient of the molal energy of vaporization divided by the molal volume, is a measure of the interatomic attractive forces. Internal pressures have been successfully applied through the regular solution theory (*17*) to the prediction of solubilities and other thermodynamic properties for many types of solutions. The application of size and internal-pressure factors to transition metal systems is discussed in detail elsewhere (*6*) and the present discussion will be limited to the effects of electronic configurations and charge transfer.

The Hume-Rothery rules imply that the free energy of a phase rises sharply beyond a limiting concentration of electrons per atom. For the bcc structure, this limit is about 1.5 electrons per atom for nontransition metals. Engel (*4*) has extended the Hume-Rothery rules to transition metals by noting that the same rules are applicable to both types of metals if *d* electrons are not included in the electron-per-atom count. A considerable number of electron phases have now been characterized as being restricted to a limited range of *s,p* electrons per atom.

The behavior of electron phases is illustrated in Fig. 4. The complete diagram, including temperature variation, would require a six-dimensional plot; Fig. 4 represents a projection to a two-dimensional diagram (*6*). Each point corresponds to an alloy composition, with the abscissa giving the atomic percent of molybdenum and with the right ordinate corresponding to the average electron-per-atom contribution of the metals on the right-hand side, which varies from six for tungsten to ten for platinum. For example, a horizontal line at the osmium position (eight electrons per atom) represents a projection of the binary molybdenum-osmium system along the temperature axis so that the composition range of each phase region represents the maximum extent at the optimum temperature. Thus the bcc phase region extends from pure molybdenum to 20 atomic percent osmium; the A15 or Cr_3Si structure has a narrow composition range around Mo_3Os; the σ phase extends from 30 to 37 atomic percent osmium; the area labeled II corresponds to the hcp phase region from 48 to 100 atomic percent osmium. The areas between the indicated phase regions correspond to two-phase mixtures. A dotted area labeled B19 is an ordered phase region of AuCd structure which separates from the hcp phase at low temperature. A horizontal line drawn halfway between rhenium and osmium would intersect the sequence of phase regions resulting from adding molybdenum to an equimolal mixture of rhenium and osmium or an equimolal mixture of tungsten, rhenium, osmium, and iridium. The elements on the right side have been chosen from the adjoining elements of the same transition series to minimize the effect of variation of atomic size and of internal pressure and thus to isolate the effect of electron concentration. If tungsten, rhenium, osmium, iridium, and platinum are mixed in varying proportions to yield an average concentration of valence electrons of 7.5 electrons per atom, then the alloy behavior upon adding molybdenum to this mixture is expected to be approximately the same as indicated by the horizontal line midway between rhenium and osmium. This type of plot, which emphasizes the primary role of average electron concentration, represents a maximum of information that can be presented in two dimensions and is in close agreement with all the reliable data available. As the average electron concentration is increased by adding face-centered cubic (fcc) iridium or platinum to bcc molybdenum, a wide region of structure II (hcp) parallels the sequence I, II, III shown in Table 1 as the electron concentration in pure metals is increased from that of molybdenum and tungsten to that of rhenium and iridium.

If lines of equal electron concentration per atom were plotted across the diagram, they would be curved lines sloping for seven electrons per atom; for example, from rhenium on the right to a 25 percent platinum, 75 percent molybdenum alloy on the left. The electron phases such as structures σ, χ, I, II, and III have boundaries which tend along isoelectronic lines. This must be due to a rapid increase in free energy at limiting electron concentrations. The actual phase limit will then be determined by thermodynamic considerations which must take into account the temperature, the thermodynamic activities in the saturating phase, and the other necessary thermodynamic criteria (*6*). Phase guides of the type shown in Fig. 4 not only condense a large amount of information into compact form, but also serve as guides to the prediction of phase diagrams which have not yet been studied. The need for such predictive ability is emphasized by the physical impossibility of experimental determination of the over 2×10^9 multicomponent phase diagrams resulting from combinations of only 30 metals. Reliable predictions of over 10^9 of the multicomponent phase diagrams of the transition metals may be made with the aid of plots like Fig. 4 together with the tables and text (*6*).

Although it is the *s* and *p* electrons that determine the long-range structure according to the Engel theory (*4*, *6*, *8*), the *d* electrons through their short-range bonding play a decisive role in determining stability. The metals at the left of the transition series use all of their valence electrons in bonding, but they do have vacant *d* and *p* orbitals that are unused. On the right side, the transition metals use all of their *d* orbitals, but the internal pairing required by the Pauli principle makes some of the *d* electrons unavailable for bonding. On this basis, an alloy of zirconium and platinum should be unusually stable. One would expect transfer of *d* electrons from platinum (d^7sp^2) to low-lying vacant orbitals of zirconium. For every electron transferred with resulting unpairing of two internally paired electrons, two electrons are made available for bonding by pairing between atoms. This prediction has now been confirmed by the demonstration that carbides of the metals at the left of the second and third transition series, which are the most stable carbides known, are decomposed by metals of the platinum group to produce compounds such as $ZrPt_3$ with heats of formation ranging up to 80 kilocalories per mole (*18*).

A particularly simple illustration of the role of *d* electrons is the effect of small additions of transition metal solutes upon the equilibrium between the bcc and hcp phases of the fourth-group transition metals. Any transition metal with three or more unpaired *d* electrons would not be able to make as good use of these electrons in bonding when surrounded by d^2sp zirconium atoms (hcp) as when surrounded by d^3s zirconium atoms (bcc). In confirmation, all transition metals to the right of the fourth group, with no known exception, stabilize the bcc phases of titanium, zirconium, and hafnium relative to the hcp phases.

The above illustrations point out the importance of applying the Engel correlation to obtain the distribution of valence electrons between *d* and *s,p*. In addition to unifying the Hume-Rothery rules and related rules for electron phases, as applied to alloys either of only nontransition metals or of only transition metals, the value of the Engel correlation can be particularly shown by systems containing both types of metals (*8*).

Summary

The same principles of chemical bonding that have been applied to nonmetals and compounds generally can be applied to metals including the transition metals. The Engel correlation between electronic configurations and crystal structures of metals has been combined with spectroscopic data for the gaseous transition metal atoms to permit calculation of thermodynamic properties of the different crystalline forms of the transition metals, both stable and metastable. Recognition of the relatively poor overlap of bonding *d* orbitals allows prediction of the effect of pressure upon relative stabilities of different crystal structures of the transition metals and also leads to an understanding of the limited occurrence of ferromagnetism among the transition metals. The concept of Hume-Rothery phases or electron phases can be applied to transition and nontransition metals in a unified manner. The above procedures have been used to predict the crystal structures and maximum composition ranges of the intermediate phases of over 10^9 of the multicomponent phase diagrams of the transition metals.

References and Notes

1. Relatively elementary comparisons of the two methods are given by J. W. Linnett, *Wave Mechanics and Valency* (Methuen, London, 1966); C. A. Coulson, *Valence* (Oxford Univ. Press, Oxford, ed. 2, (1963); R. S. Mulliken, *Science* **157**, 13 (1967).
2. H. C. Longuet-Higgins, *Proc. Phys. Soc. London* **60**, 270 (1948); C. A. Coulson, *Valence* (Oxford Univ. Press, Oxford, ed. 2, 1963), pp. 154, 274, and 332.
3. L. Pauling, *Proc. Roy. Soc. London Ser. A* **196**, 343 (1949); *The Nature of the Chemical Bond* (Cornell Univ. Press, Ithaca, N.Y., ed. 3, 1960).
4. N. Engel, *Ingenioeren* **N101**(1939), M1 (1940); *Haandogi Metalläre* (Selskabet for Metalforskning, Copenhagen, 1945); *Kemisk Maandesblad* **30**(5), 53; (6), 75; (8), 97; (9), 105; (10), 114 (1949); *Powder Met. Bull.* **7**, 8 (1954); *Amer. Soc. Metals, Trans. Quart.* **57**, 610 (1964); *Acta Met.* **15**, 557 (1967).
5. C. E. Moore, *Atomic Energy Levels* [Government Printing Office, Washington, D.C., vol. 1 (1949), vol. 2 (1952), vol. 3 (1958)].
6. L. Brewer, in *High-Strength Materials*, V. F. Zackay, Ed. (Wiley, New York, 1965), pp. 12–103.

→ S. L. Altmann, C. A. Coulson, W. Hume-Rothery, *Proc. Roy. Soc. London Ser. A* **240**, 145 (1957).

8. L. Brewer, in *Phase Stability in Metals and Alloys*, P. Rudman, J. Stringer, R. I. Jaffee, Eds. (McGraw-Hill, New York, 1967), pp. 39–61, 241–9, 344–6, and 560–8.
9. D. T. Peterson and R. P. Colburn, *J. Phys. Chem.* **70**, 468 (1966).
10. C. E. Myers, *J. Chem. Educ.* **43**, 303 (1966).
11. W. Hume-Rothery, *The Metallic State* (Oxford Univ. Press, Oxford, 1931); *Structures of Metals and Alloys* (Institute of Metals, London, 1936).
12. J. Tellinghuisen, personal communication.
13. Tabulated data (*6*, *8*) have been brought up to date with values from R. Hultgren, R. L. Orr, K. K. Kelley, *Supplement to Selected Values for the Thermodynamic Properties of Metals and Alloys* (University of California, Berkeley, 1964–8); D. D. Wagman, W. H. Evans, I. Halow, V. B. Parker, S. M. Bailey, R. H. Schumm, *NBS Technical Notes 270-3* (Government Printing Office, Washington, D.C., 1968). The data for phosphorus are for the triclinic red modification.
14. D. T. Peterson and V. G. Fattore, *J. Phys. Chem.* **65**, 2062 (1961).
15. P. S. Rudman, *Trans. AIME* **233**, 864 (1965).
16. C. S. Barrett, *Acta Cryst.* **9**, 671 (1956).
17. J. H. Hildebrand and R. L. Scott, *Solubility of Nonelectrolytes* (Reinhold, New York, ed. 3, 1950); *Regular Solutions* (Prentice-Hall, Englewood Cliffs, N.J., 1962).
18. L. Brewer, *Acta Met.* **15**, 555 (1967).
19. Sponsored by the AEC.